JAMA Neurology | Original Investigation

Staging β-Amyloid Pathology With Amyloid Positron Emission Tomography

Niklas Mattsson, MD, PhD; Sebastian Palmqvist, MD, PhD; Erik Stomrud, MD, PhD; Jacob Vogel; Oskar Hansson, MD, PhD

IMPORTANCE Different brain regions appear to be involved during β-amyloid (Aβ) accumulation in Alzheimer disease (AD), but a longitudinally valid system to track Aβ stages in vivo using positron emission tomography (PET) is lacking.

OBJECTIVE To construct a longitudinally valid in vivo staging system for AD using amyloid PET.

DESIGN, SETTING, AND PARTICIPANTS Longitudinal multicenter cohort study using data accessed on August 20, 2018, from the Alzheimer's Disease Neuroimaging Initiative database of scans performed from June 9, 2010, to July 12, 2018, from 741 persons: 304 without cognitive impairment, 384 with mild cognitive impairment, and 53 with AD dementia. Cerebrospinal fluid (CSF) Aβ42 and fluorine 18–labeled florbetapir (^{18}F-florbetapir) data were used to determine early, intermediate, and late regions of Aβ accumulation. β-Amyloid stages ranging from 0 to 3 were constructed using these composites. Each subsequent stage required involvement of more advanced regions. Patients were followed up at 2, 4, and 6 years. Replication and validation were conducted using an independent cohort (Swedish BioFINDER) and gene expression information from the Allen Human Brain Atlas database. Analyses were conducted August 21, 2018, to May 24, 2019.

MAIN OUTCOMES AND MEASURES The main outcome was change in stage. Stages were compared for diagnosis, CSF biomarkers of tau, and longitudinal atrophy, cognitive measures, and regional gene expression. Transitions between stages were tested using longitudinal ^{18}F-florbetapir data.

RESULTS Among 641 participants with CSF Aβ42 data and at least two ^{18}F-florbetapir scans, 335 (52.3%) were male. The early region of Aβ accumulation included the precuneus, posterior cingulate, isthmus cingulate, insula, and medial and lateral orbitofrontal cortices. The late region included the lingual, pericalcarine, paracentral, precentral, and postcentral cortices. The intermediate region included remaining brain regions with increased accumulation rates. In 2072 PET scans from 741 participants, 2039 (98.4%) were unambiguously staged. At baseline, participants with stage 0 (n = 402) had a 14.7% (95% CI, 11.2%-18.1%) probability of progression to a higher stage; stage 1 (n = 21), 71.4% (95% CI, 50.0%-90.9%); and stage 2 (n = 79), 53.1% (95% CI, 42.2%-64.0%). Seven of the 741 participants (0.9%) reverted to a lower stage. Higher stages were associated with lower CSF Aβ42 concentrations (from stage 1 at baseline), greater CSF P-tau (from stage 1) and CSF T-tau (from stage 2), and accelerated cognitive decline (from stage 2) and atrophy (from stage 3), even when adjusting for clinical diagnosis. Key findings were replicated in the BioFINDER cohort (N = 474). The regions of different stages differed by gene expression profiles when using the transcriptome from the Allen Human Brain Atlas, especially involving genes associated with voltage-gated ion channel activity especially involving genes associated with voltage-gated ion channel activity, but also blood circulation, axon guidance, and lipid transportation.

CONCLUSIONS AND RELEVANCE Results of this study suggest that this robust staging system of Aβ accumulation may be useful for monitoring patients throughout the course of AD. Progression through stages may depend on underlying selective vulnerability in different brain regions.

JAMA Neurol. 2019;76(11):1319-1329. doi:10.1001/jamaneurol.2019.2214
Published online July 17, 2019.

Supplemental content

Author Affiliations: Clinical Memory Research Unit, Faculty of Medicine, Lund University, Lund, Sweden (Mattsson, Palmqvist, Stomrud, Hansson); Department of Neurology, Skåne University Hospital, Lund, Sweden (Mattsson, Palmqvist); Wallenberg Center for Molecular Medicine, Lund University, Lund, Sweden (Mattsson); Memory Clinic, Skåne University Hospital, Malmö, Sweden (Hansson); Montreal Neurological Institute and Hospital, Montreal, Quebec, Canada (Vogel).

Corresponding Authors: Niklas Mattsson, MD, PhD (niklas.mattsson@med.lu.se); Oskar Hansson, MD, PhD, Clinical Memory Research Unit, Lund University, Simrisbanvagen 14, Malmö, CA 21224, Sweden (oskar.hansson@med.lu.se).

Alzheimer disease (AD) is characterized by accumulation of β-amyloid (Aβ), which likely starts before cognitive impairment, precedes neurodegeneration, and continues in the symptomatic stage.[1,2] The accumulation may affect different regions of the brain at different time points,[3,4] making it possible to characterize Aβ deposition in a staging system in vivo, as has been done with postmortem neuropathologic studies of the brain (eg, Thal phases).[3,4] Neuropathologic studies cannot directly be applied to in vivo assessments using Aβ position-emission tomography (PET), because Aβ binding may differ between neuropathology staining and PET uptake, where the Aβ PET tracer predominantly binds to the fibrillary conformation of Aβ.[5,6] A modern Aβ staging system can also leverage that cerebrospinal fluid (CSF) measurements of the Aβ42 peptide may identify Aβ accumulation earlier than Aβ PET.[7-9] Combinations of PET and CSF studies may be used to identify regions where accumulation of Aβ fibrils begin (by studying individuals who are Aβ42 positive in CSF studies but still Aβ PET negative) and regions that are affected later in the disease.[10] We used this method to construct a staging system, which we validated by examining the prevalence of unambiguously classified participants, differences in cognition by stage, biomarkers, and imaging, regional gene expression, and longitudinal transition because it is crucial to demonstrate that individuals are at risk for transitions from lower to higher stages.

Key Points

Question Can a longitudinally valid in vivo β-amyloid staging system be constructed for Alzheimer disease?

Findings In this multicenter longitudinal cohort study, a 4-level staging system using fluorine 18–labeled florbetapir positron emission tomography was defined using a combination of cerebrospinal fluid and positron emission tomography data. The β-amyloid stages had distinct associations with cerebrospinal fluid tau biomarkers, atrophy, and cognitive decline, had longitudinal validity in an analysis of transitions between stages, and were associated with distinct gene expression profiles; key results were validated in a replication cohort using fluorine 18-labeled flutemetamol positron emission tomography.

Meaning Results of this study suggest that a novel β-amyloid staging system using positron emission tomography, in which stages are associated with different biological and clinically meaningful end points, can be used to track progression of Alzheimer disease longitudinally.

Methods

This study followed the Strengthening the Reporting of Observational Studies in Epidemiology (STROBE) reporting guideline. Data were obtained from the Alzheimer's Disease Neuroimaging Initiative (ADNI) database (http://adni.loni.usc.edu). Participants in the ADNI have been recruited from more than 50 sites across the United States and Canada. Up-to-date information is available at http://www.adni-info.org. For the present study, we used data accessed from the ADNI database on August 20, 2018, from scans performed from June 9, 2010, to July 12, 2018. For replication and validation, we used an independent cohort (Swedish BioFINDER; scans performed July 6, 2009, to December 17, 2014) and gene expression information from the Allen Human Brain Atlas database (http://human.brain-map.org/; data accessed January 25, 2019). Analyses were conducted August 21, 2018, to May 24, 2019. All study participants gave written informed consent. Regional ethical committees of all institutions involved approved the study.

Participants

Our main cohort from the ADNI database consisted of all cognitively unimpaired (CU) control participants, patients with mild cognitive impairment (MCI), and patients with AD dementia for whom at least 2 fluorine 18-labeled florbetapir (^{18}F-florbetapir) scans (N = 741) were available. Inclusion and exclusion criteria for ADNI have been described elsewhere.[11] Briefly, all participants were aged between 55 and 90 years, had 6 or more years of education, were fluent in Spanish or English, and had no clinically significant neurologic disease other than AD. Cognitively unimpaired control participants had Mini-Mental State Examination (MMSE)[12] scores of 24 or greater (total possible range, 0-30, with higher scores indicating better performance) and Clinical Dementia Rating (CDR)[13] scores of 0 (total possible range, 0-3, with higher scores indicating worse functioning). Patients with MCI had MMSE scores of 24 or greater, objective memory loss tested by delayed recall of the Wechsler Memory Scale Logical Memory II, CDR scores of 0.5, and preserved activities of daily living. Patients with AD dementia fulfilled the National Institute of Neurological and Communicative Disorders and Stroke and the Alzheimer's Disease and Related Disorders Association criteria for probable AD (dementia, progressive impairment, and absence of other diseases capable of producing dementia)[14] and had MMSE scores of 20 to 26 and CDR scores of 0.5 to 1.0. We used MMSE[12] for global cognition and cognitive composites for memory[15] and executive function.[16] Cerebrospinal fluid samples in the ADNI were analyzed for CSF Aβ42, total tau (T-tau) and phosphorylated tau (P-tau) using the AlzBio3 assays (Fujirebio) on the xMAP platform (Luminex).[17]

Magnetic Resonance Imaging

Structural brain images were acquired using 3-T magnetic resonance imaging scanners with T1-weighted scans. FreeSurfer version 5.1 (http://surfer.nmr.mgh.harvard.edu) was used for regional quantifications according to the 2010 Desikan-Killany atlas.[18] We used cortical thickness in a metaregion of interest involving the entorhinal, inferior temporal, middle temporal, and fusiform cortices, correcting for surface area (temporal composite).[19]

^{18}F-Florbetapir PET Imaging

β-Amyloid PET imaging in the ADNI was performed using ^{18}F-florbetapir PET.[20] A composite reference region suitable for longitudinal analyses was used to calculate standardized uptake value ratios (SUVRs).[21] A neocortical composite region consisting of the weighted mean uptake in the frontal, lateral pa-

rietal, lateral temporal, and cingulate regions was used for global Aβ PET.[22] FreeSurfer segmented SUVRs were used for regional analyses.

Aβ Staging

The composite regions were defined using participants with both CSF and PET data. Each individual was classified as Aβ positive or negative on CSF and Aβ positive or negative on PET at baseline. Cerebrospinal fluid positivity was defined as CSF Aβ42 less than 192 ng/L.[17] Positron emission tomography positivity was defined as global neocortical ^{18}F-florbetapir uptake greater than 0.826 SUVR, based on mixture modeling analysis.[23] This process resulted in 4 groups: CSF-negative/PET-negative (n = 288, nonaccumulators), CSF-positive/PET-negative (n = 69, early accumulators), CSF-negative/PET-positive (n = 10, discordant), and CSF-positive/PET-positive (n = 274, late accumulators) (eTable 1 in the Supplement). Regional ^{18}F-florbetapir uptake rates (using baseline and 2-year scans) were compared (using the mean SUVR from the left and right hemispheres) between groups. We included only regions that had significantly increased ^{18}F-florbetapir uptake rates in CSF-positive/PET-positive (late accumulators) compared with CSF-negative/PET-negative (nonaccumulators) (eTable 2 in the Supplement). We contrasted CSF-positive/PET-negative (early accumulators) with CSF-negative/PET-negative (nonaccumulators) to identify regions in the early composite (eTable 3 in the Supplement)[10] and compared CSF-positive/PET-positive (late accumulators) with CSF-positive/PET-negative (early accumulators) to identify regions in the late composite (eTable 4 in the Supplement). Remaining regions with increased rates in CSF-positive/PET-positive (late accumulators) compared with CSF-negative/PET-negative (nonaccumulators) were merged into the intermediate composite. Cut points for composite positivity were generated in the CSF Aβ42-negative population, at the mean level plus 2 SDs of the uptake (eFigure in the Supplement).

Scans were assigned to stage 0 if they were negative in all composites, stage 1 if they were positive in the early composite, stage 2 if they were positive in the early and intermediate composites, or stage 3 if they were positive in all 3 composites, or were considered unstageable if they did not follow the staging rules (eTable 5 in the Supplement).

Replication

The replication cohort from the Swedish BioFINDER study included 306 CU control participants and 168 with MCI using cross-sectional PET imaging with fluorine 18-labeled flutemetamol (^{18}F-flutemetamol),[24] CSF biomarkers (Elecsys assays for Aβ42, T-tau, and P-tau; Roche Diagnostics GmbH),[25] cognitive testing (longitudinal MMSE scores), and magnetic resonance imaging of the brain (for mean temporal cortical thickness). We applied the early, intermediate, and late regions from the ADNI sample. To define composite cut points for ^{18}F-flutemetamol uptake, we identified a group of CSF Aβ42-negative CU participants in the BioFINDER sample (using CSF Aβ42 > 1100 ng/L[25]). The ^{18}F-flutemetamol composites had possible bimodal distributions, with a few cases with elevated ^{18}F-flutemetamol uptake; therefore, cut points were defined using mixture modeling (eFigure in the Supplement).

Gene Expression Analysis

Brain gene expression information from the Allen Human Brain Atlas database (http://human.brain-map.org/) was used to explore biological signals corresponding to the early, intermediate, and late composites. A cross-validated, consensus-based, class-balanced ordinal logistic regression classifier was trained to identify the location of tissue samples extracted from early, intermediate, and late regions and was validated on unseen test data. Genewise classifier weights were submitted to a leading-edge gene set enrichment analysis using Gene Set Enrichment Analysis (GSEA) software (Broad Institute, UC San Diego)[26] to identify enriched biological pathways associated with the genes that contributed to the region classifier. Further details can be found in the eAppendix in the Supplement.

Statistical Analysis

Longitudinal regional ^{18}F-florbetapir rates were compared 1 to 1 between CSF/PET groups with linear regression, adjusted for age, sex, and time between PET scans. Longitudinal data for global ^{18}F-florbetapir SUVR, longitudinal MMSE, memory composite, executive composite, and temporal lobe thickness measures were modeled in linear mixed-effects models. Participant-specific slopes were compared between Aβ stages in linear regression models, adjusted for age, sex, education, and clinical diagnosis (CSF biomarkers, with baseline data only, were compared in linear regression models with the same covariates). Transitions between stages were tested using longitudinal data with 95% CIs, using a bootstrap procedure (1000 iterations).

In the replication cohort, only cross-sectional PET data were available. We tested for stage differences in cross-sectional CSF biomarkers and temporal lobe thickness using linear regression, and for longitudinal measures of MMSE using linear mixed-effects models, adjusted for the same covariates as the main analyses.

Two-sided *P* values were corrected for multiple comparisons, when indicated. $P < .05$ was considered statistically significant. All statistical analyses were performed using R, version 3.4.4 (R Foundation).

Results

Aβ Composites

Six hundred forty-one participants with CSF Aβ42 data and at least two ^{18}F-florbetapir scans were classified into CSF/PET groups. Of the 641, 335 (52.3%) were male; further demographic data are available in eTable 1 in the Supplement. Uptake rates of ^{18}F-florbetapir were compared. Six regions with greater rates in early accumulators than in nonaccumulators (precuneus, posterior cingulate, isthmus cingulate, insula, and medial and lateral orbitofrontal cortices) were merged into the early composite (**Figure 1**A; cut point, 0.8395 SUVR). Five regions with greater rates in late accumulators than in early ac-

Figure 1. β-Amyloid (Aβ) Stages of Alzheimer Disease by Longitudinal Fluorine 18–Labeled Florbetapir (^{18}F-Florbetapir) Positron Emission Tomography (PET)

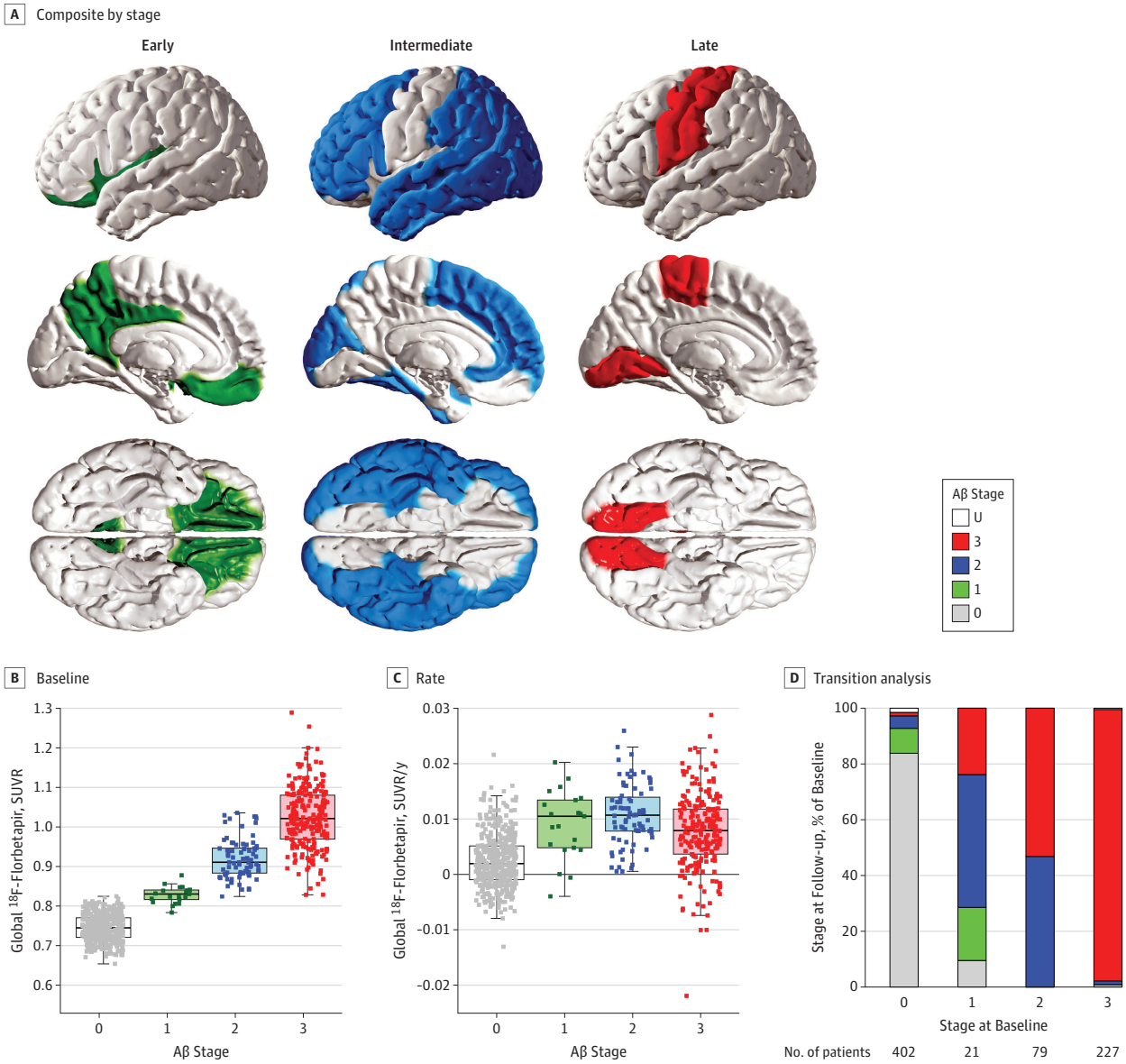

A, Early (positive in stage 1), intermediate (positive in stage 2), and late (positive in stage 3) composites (eTables 2-4 in the Supplement). B, Baseline global neocortical ^{18}F-florbetapir by Aβ stage. C, shows the rates of global neocortical ^{18}F-florbetapir by Aβ stage. Baseline and rates are participant-specific intercepts and slopes from a linear mixed effects model with all available longitudinal data (Table 2 provides numerical details, including statistical comparisons). D, Intraindividual Aβ stage transitions from baseline to follow-up, using the last available scan for each participant for follow-up. For each baseline stage, data are expressed as proportion of participants for each of the possible follow-up stages. The 12 participants who were unstageable at baseline are not shown in the figure. Table 3 shows numerical details, including 95% CIs for the proportions. SUVR indicates standardized uptake value ratio; U, unstageable.

cumulators (lingual, pericalcarine, paracentral, precentral, and postcentral cortices) were merged into the late composite (Figure 1A; cut point, 0.8478 SUVR). The remaining regions, which had greater rates in late accumulators compared with nonaccumulators but not compared with early accumulators, were merged into the intermediate composite (Figure 1A; cut point, 0.8168 SUVR) (banks of the superior temporal sulcus, caudal middle frontal, cuneus, frontal pole, fusiform, inferior parietal, inferior temporal, lateral occipital, middle temporal, parahippocampal, pars opercularis, pars orbitalis, pars triangularis, putamen, rostral anterior cingulate, rostral middle frontal, superior frontal, superior parietal, superior temporal, and supramarginal regions).

Aβ Stages

The second part of the study, during which stages were assigned, included 741 participants. Of 2072 scans, 2039 (98.4%) were unambiguously staged (eTable 6 in the Supplement).

Table 1. Demographic Features by Diagnostic Group

Patient Characteristic	Mean (SD)[a]		
	CU	MCI	AD
No.	304	384	53
Age, y	74.4 (6.6)	72.0 (7.8)	76.8 (7.1)
Sex, No. (%)			
Male	148 (48.7)	218 (56.8)	29 (54.7)
Female	156 (51.3)	166 (43.2)	24 (45.3)
Education, y	16.5 (2.7)	16.2 (2.7)	15.8 (3.0)
No. of scans			
2	105	170	46
3	127	126	6
4	67	85	0
5	5	3	1
MMSE Score[b]			
Baseline	29.04 (0.6)	28.29 (1.1)	25.79 (2.6)
Rate, y	−0.104 (0.252)	−0.469 (0.748)	−1.691 (0.933)
Memory Composite, z[c]			
Baseline	1.17 (0.52)	0.51 (0.69)	−0.31 (0.70)
Rate, y	−0.038 (0.061)	−0.083 (0.105)	−0.19 (0.085)
Executive Composite, z[d]			
Baseline	0.98 (0.64)	0.54 (0.75)	−0.19 (0.99)
Rate, y	−0.03 (0.079)	−0.07 (0.114)	−0.21 (0.125)
Temporal Cortex, mm			
Baseline	2.79 (0.12)	2.74 (0.16)	2.52 (0.18)
Rate, y	−0.017 (0.013)	−0.023 (0.021)	−0.051 (0.025)
CSF, ng/L			
Aβ42	202.8 (50.1)	178.4 (52.6)	143.5 (46.7)
T-tau	67.6 (33.0)	84.9 (50.1)	131.5 (58.8)
P-tau	35.0 (18.0)	40.5 (25.0)	58.7 (31.8)
Aβ PET[e]			
Baseline >0.826 (yes/no)	80/224	196/188	44/9
Baseline, SUVR	0.804 (0.108)	0.872 (0.136)	0.995 (0.141)
Rate, SUVR/y	0.0047 (0.0064)	0.0052 (0.0063)	0.0065 (0.0077)
Follow-up time, y[f]	4.1 (1.6)	3.9 (1.7)	2.4 (1.0)
Baseline Aβ Stage, No. (%)			
0	214 (70.4)	179 (46.6)	9 (17.0)
1	11 (3.6)	10 (2.6)	0 (0)
2	24 (7.9)	53 (13.8)	2 (3.8)
3	50 (16.4)	135 (35.2)	42 (79.2)
Unstageable	5 (1.6)	7 (1.8)	0 (0)

Abbreviations: Aβ, β-amyloid; AD, Alzheimer disease with dementia; CSF, cerebrospinal fluid; CU, cognitively unimpaired; ^{18}F-florbetapir, fluorine 18–labeled florbetapir; MCI, mild cognitive impairment; MMSE, Mini-Mental State Examination; PET, positron emission tomography; P-tau, phosphorylated tau; SUVR, standardized uptake value ratio; T-tau, total tau.

[a] Continuous data are mean (SD).

[b] Possible MMSE scores range from 0 to 30, with higher scores indicating better performance.[12]

[c] The memory composite is calculated from memory tests in MMSE, Alzheimer's Disease Assessment Schedule, Rey Auditory Verbal Learning Test, and logical memory (immediate and delayed) as described by Crane et al.[15]

[d] The executive composite is calculated from category fluency animals, category fluency vegetables, Trail Making Test parts A and B, digit span backwards, Wechsler Adult Intelligence Scale R digit symbol substitution, number cancellation, and 5 clock-drawing items, as described by Gibbons et al.[16]

[e] Aβ PET is the global neocortical ^{18}F-florbetapir composite.

[f] Follow-up time is from the first to the final scan.

Different stages had different prevalence among the diagnostic groups (**Table 1**).[12,15,16] Most CU participants were in stage 0, most participants with MCI were in stage 0 or stage 3, and most participants with AD dementia were in stage 3. Stages 1 and 2 were mainly seen in CU participants and those with MCI.

Demographic features by stage are shown in **Table 2**.[12,15,16] Among the 421 participants who were Aβ negative according to global ^{18}F-florbetapir uptake at baseline, 402 (95.5%) were classified as stage 0, 10 (2.4%) as stage 1, 1 (0.2%) as stage 2, and 8 (1.9%) were unstageable. Among the 320 who were Aβ positive according to the global ^{18}F-florbetapir uptake, 11 (3.4%) were classified as stage 1, 78 (24.4%) as stage 2, 227 (70.9%) as stage 3, and 4 (1.3%) were unstageable.

The baseline global ^{18}F-florbetapir SUVR increased gradually from stage 0 to stage 3, whereas the ^{18}F-florbetapir uptake rates were greatest in stage 2 (Table 2, Figure 1B, C). Cerebrospinal fluid biomarkers shifted toward more pathologic levels from stage 1 (for CSF Aβ42 and P-tau) or from stage 2 (for CSF T-tau). Cognitive decline accelerated in stage 2 and atrophy accelerated in stage 3.

Longitudinal Analysis

The main analysis of longitudinal transitions between stages used the first and last available scan for each participant (**Figure 2** and **Table 3**). Participants in stage 0 had a 14.7% (59 of 402) risk (95% CI, 11.2%-18.1%) of progressing to a higher

Table 2. Baseline Aβ Stage Characteristics

Variable	Stage[a]					*P* Value					
	0	1	2	3	Unstageable	0 vs 1	0 vs 2	0 vs 3	1 vs 2	1 vs 3	2 vs 3
No. (%)	402 (54.3)	21	79	227	12	NA	NA	NA	NA	NA	NA
Diagnosis, No.											
CU	214	11	24	50	5	.77	< .001	< .001	.15	.0031	.0018
MCI	179	10	53	135	7						
AD dementia	9	0	2	42	0						
Age, y	72.6 (7.6)	71 (6.4)	74.6 (8.6)	74.5 (6.5)	70.7 (7.8)	.34	.04	.0018	.08	.02	.94
Sex, No.											
Male	221	11	48	113	2	.99	.41	.24	.66	> .99	.12
Female	181	10	31	114	10						
Education, y	16.5 (2.6)	16.8 (2.9)	16.1 (2.7)	15.8 (2.8)	16.3 (2.7)	.65	.20	< .001	.32	.11	.31
No. of scans											
2	142	8	34	132	5	.93	.36	< .001	.90	.26	.82
3	153	8	29	67	2						
4	99	5	16	27	5						
5	8	0	0	1	0						
MMSE Score[b]											
Baseline	28.8 (1.0)	28.5 (1.0)	28.6 (1.1)	27.7 (1.8)	28.8 (0.6)	.23	.74	<.001	.37	.49	.01
Rate, y	−0.13 (0.37)	−0.05 (0.27)	−0.40 (0.52)	−0.96 (0.97)	0.02 (0.18)	.45	.01	<.001	.04	<.001	<.001
Memory Composite, *z*[c]											
Baseline	0.97 (0.64)	0.91 (0.66)	0.66 (0.65)	0.27 (0.78)	0.92 (0.54)	.40	.07	<.001	.89	.03	<.001
Rate, y	−0.031 (0.066)	−0.032 (0.080)	−0.081 (0.081)	−0.149 (0.101)	−0.024 (0.064)	.75	<.001	<.001	.07	<.001	<.001
Executive Composite, *z*[d]											
Baseline	0.89 (0.69)	0.94 (0.91)	0.62 (0.71)	0.24 (0.81)	1.00 (0.51)	.93	.23	<.001	.59	.02	.002
Rate, y	−0.024 (0.079)	−0.067 (0.087)	−0.071 (0.092)	−0.134 (0.132)	−0.002 (0.075)	.03	.002	<.001	.65	.11	<.001
Temporal Cortex, mm											
Baseline	2.79 (0.13)	2.79 (0.14)	2.74 (0.15)	2.67 (0.18)	2.84 (0.09)	.89	.17	<.001	.54	.07	.06
Rate of loss of thickness, mm/y	−0.017 (0.015)	−0.019 (0.013)	−0.022 (0.019)	−0.034 (0.023)	−0.011 (0.010)	.43	.11	<.001	.86	.04	.002
CSF, ng/L											
Aβ42	223.7 (37.9)	177.7 (32.3)	139.3 (25.6)	136.9 (26.6)	210.4 (45.7)	<.001	<.001	<.001	<.001	<.001	.76
T-tau	58.1 (24.4)	71.9 (40.5)	104.3 (49.5)	113.0 (54.3)	67.5 (28.0)	.11	<.001	<.001	.003	.004	.63
P-tau	28.2 (13.2)	41.7 (26.9)	51.1 (26.9)	54.9 (25.9)	29.1 (12.9)	.003	<.001	<.001	.06	.01	.37
Aβ PET[e]											
Baseline >0.826 (yes/ no)	0/402	11/10	78/1	227/0	4/8	NA	NA	NA	NA	NA	NA
Baseline, SUVR	0.745 (0.034)	0.828 (0.021)	0.920 (0.050)	1.023 (0.077)	0.824 (0.017)	<.001	<.001	<.001	<.001	<.001	<.001
Rate SUVR, y	0.0024 (0.0048)	0.0090 (0.0062)	0.0107 (0.0055)	0.0077 (0.0068)	0.0029 (0.0073)	<.001	<.001	<.001	.18	.37	<.001
Follow-up time, y[f]	4.1 (1.7)	4.0 (1.8)	3.8 (1.6)	3.3 (1.6)	4.6 (1.7)	.65	.13	<.001	.73	.30	.24

Abbreviations: Aβ, β-amyloid; AD, Alzheimer disease; CSF, cerebrospinal fluid; CU, cognitively unimpaired; ^{18}F-florbetapir, fluorine 18–labeled florbetapir; MCI, mild cognitive impairment; MMSE, Mini-Mental State Examination; NA, not applicable; PET, positron emission tomography; P-tau, phosphorylated tau; SUVR, standardized uptake value ratio; T-tau, total tau.

[a] Continuous data are reported as mean (SD). Diagnosis, age, sex, education and number of scans were compared between stages using χ^2 tests or linear regression, as appropriate. Baselines and rates for cognitive measures, temporal cortex, and Aβ PET are based on participant-specific intercepts and slopes from linear mixed-effects models. All continuous measures for cognition, fluid and imaging biomarkers, and follow-up time were compared 1 to 1 between stages 0 through 3 using linear regression models, adjusted for clinical diagnosis, age, sex, education. Unadjusted *P* values are shown. After Bonferroni correction (for 6 tests), *P* values are significant at $P < .0083$.

[b] Possible MMSE scores range from 0 to 30, with higher scores indicating better performance.[12]

[c] The memory composite is calculated from memory tests in the MMSE, Alzheimer's Disease Assessment Schedule, Rey Auditory Verbal Learning Test, and logical memory (immediate and delayed) as described by Crane et al.[15]

[d] The executive composite is calculated from category fluency animals, category fluency vegetables, Trail Making Test parts A and B, digit span backwards, Wechsler Adult Intelligence Scale R digit symbol substitution, number cancellation, and 5 clock-drawing items, as described by Gibbons et al.[16]

[e] Aβ PET is the global neocortical ^{18}F-florbetapir composite.

[f] Follow-up time is from the first to the final scan.

Figure 2. Predicting Amyloid Stage by Regional Gene Expression

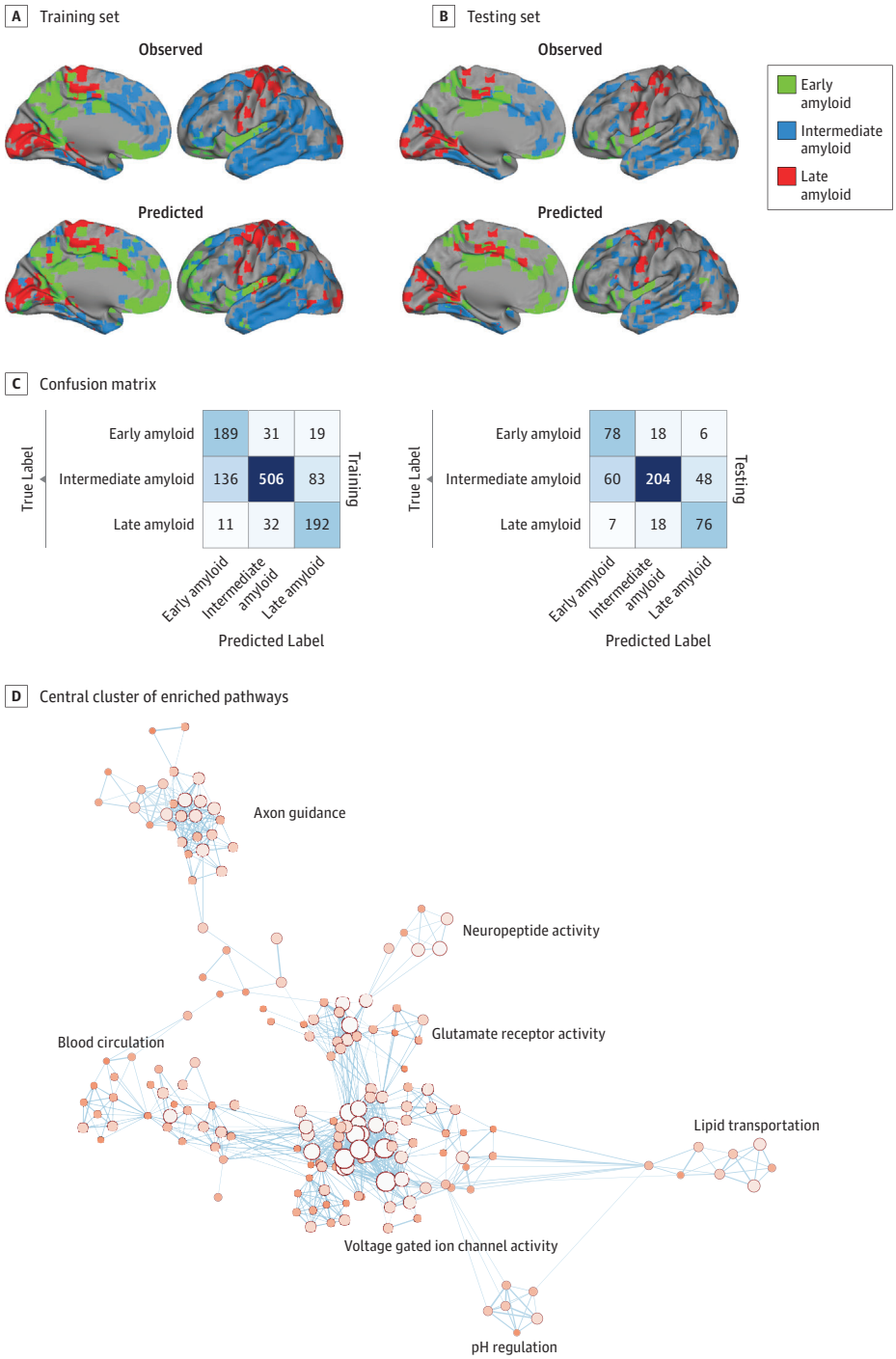

A, Surface rendering of Allen Human Brain Atlas tissue samples from the training set, colored by their observed (top row) and predicted (bottom row) labels. B, Observed and predicted labels for tissue samples from the testing set. C, Confusion matrices summarizing correct and incorrect predictions for training (left) and test (right) data. D, The primary cluster summarizing relationships between enriched (false discovery rate < 0.1) gene sets. Nodes represent individual gene sets, with node size indicating enrichment effect size based on gene set enrichment analysis leading-edge analysis. Edges represent overlapping genes within each set. Annotations represent summaries of terms composing each cluster.

stage (mainly to stage 1). Participants in stage 1 had a 71.4% (15 of 21) risk (95% CI, 50.0%-90.9%) of progressing to a higher stage. Participants in stage 2 had a 53.1% (42 of 79) risk (95% CI, 42.2%-64.0%) of progressing to a higher stage. Almost all participants in stage 3 remained at that stage during follow-up (221 of 227 [97.3%]) (95% CI, 95.2%-99.1%). Ten par-

Table 3. Longitudinal Aβ Stage Transition Analysis

Aβ Stage at Baseline, No.	Aβ Stage at Follow-up, No. (%) [95% CI]				
	0	1	2	3	Unstageable
Transition Analysis: Baseline to Last Available Aβ Stage (n = 741)					
No. of patients	345	41	71	275	9
0 (n = 402)	337 (83.8%) [80.1-87.3][a]	36 (9.0%) [6.2-11.8][a]	18 (4.5%) [2.6-6.5][a]	5 (1.2%) [0.3-2.5][a]	6 (1.5%) [0.5-2.8]
1 (n = 21)	2 (9.5%) [0.0-23.5]	4 (19.0%) [4.5-39.1][a]	10 (47.6%) [24.1-68.8][a]	5 (23.8%) [4.8-43.5][a]	0
2 (n = 79)	0	0	37 (46.8%) [36.0-57.8][a]	42 (53.2) [42.2-64.0][a]	0
3 (n = 227)	2 (0.9%) [0.0-2.5]	0	3 (1.3%) [0.0-3.0]	221 (97.4%) [95.5-99.1][a]	1 (0.4%) [0.0-1.4]
Unstageable (n = 12)	4 (33.3%) [8.3-61.5]	1 (8.3%) [0.0-28.6]	3 (25.0%) [0.0-28.6]	2 (16.7%) [0.0-53.3]	2 (16.7%) [0.0-42.9]
Transition Analysis: Baseline to 2-y Follow-up (n = 666)					
No. of patients	338	26	59	232	11
0 (n = 361)	334 (92.5%) [89.7-95.2][a]	19 (5.3%) [3.2-7.9][a]	5 (1.4%) [0.3-2.7][a]	1 (0.3%) [0.0-0.9][a]	2 (0.6%) [0.0-1.4]
1 (n = 18)	1 (5.6%) [0.0-18.8]	7 (38.9%) [16.7-62.5][a]	7 (38.9%) [15.4-61.5][a]	3 (16.7%) [0.0-35.3][a]	0
2 (n = 71)	0	0	43 (60.6%) [48.6-72.5][a]	27 (38.0%) [26.8-49.4][a]	1 (1.4%) [0.0-4.9]
3 (n = 206)	1 (0.5%) [0.0-1.7]	0	3 (1.5%) [0.0-3.4]	200 (97.1%) [94.9-99.1][a]	2 (1.0%) [0.0-2.5]
Unstageable (n = 10)	2 (20.0%) [0.0-50.0]	0	1 (10.0%) [0.0-30.9]	1 (10.0%) [0.0-33.3]	6 (60.0%) [25.0-91.0]
Transition Analysis: Baseline to 4-y Follow-up (n = 369)					
No. of patients	203	17	36	110	3
0 (n = 228)	198 (86.8%) [82.2-90.9][a]	16 (7.0%) [3.9-10.5][a]	11 (4.8%) [2.3-7.8][a]	1 (0.4%) [0.0-1.4][a]	2 (0.9%) [0.0-2.3]
1 (n = 12)	2 (16.7%) [0.0-44.4]	0[a]	7 (58.3%) [25.0-87.5][a]	3 (25.0%) [0.0-53.8][a]	0
2 (n = 39)	0	0	16 (41.0%) [25.0-57.1][a]	23 (58.9%) [42.9-75.0][a]	0
3 (n = 85)	1 (1.2%) [0.0-4.0]	0	1 (1.2%) [0.0-3.7]	83 (97.6%) [94.0-100.0][a]	0
Unstageable (n = 5)	2 (40.0%) [0.0-100.0]	1 (20.0%) [0.0-66.7]	1 (20.0%) [0.0-66.7]	1 (0.0%) [0.0-0.0]	1 (20.0%) [0.0-61.2]
Transition Analysis: Baseline to 6-y Follow-up (n = 139)					
No. of patients	79	13	7	36	5
0 (n = 99)	76 (76.8%) [68.6-85.2][a]	12 (12.1%) [6.0-18.8][a]	5 (5.1%) [1.0-9.6][a]	1 (1.0%) [0.0-3.2][a]	5 (5.1%) [1.0-10.1]
1 (n = 3)	1 (33.3%) [0.0-100.0]	0[a]	0[a]	2 (66.7%) [0.0-100.0][a]	0
2 (n = 10)	0	0	1 (10.0%) [0.0-33.3][a]	9 (90.0%) [66.7-100.0][a]	0
3 (n = 23)	0	0	0	23 (100.0%) [100.0-100.0][a]	0
Unstageable (n = 5)	2 (40.0%) [0.0-80.3]	1 (20.0%) [0.0-66.7]	1 (20.0%) [0.0-66.7]	1 (20.0%) [0.0-66.7]	0

Abbreviation: Aβ, β-amyloid.

[a] Transitions that follow the staging system (ie, remain in baseline stage or progress to a higher stage).

ticipants were unstageable at baseline (1.3%), 7 at the final stage (0.9%), and 2 at both stages (0.3%) and 7 (0.9%) reverted from a higher to a lower stage at follow-up. A sensitivity analysis without the participants with AD dementia produced similar results: Participants in stage 0 had a 14.7% (58 of 393) risk of progressing to a higher stage (mainly to stage 1). Participants in stage 1 had a 71.4% (15 of 21) risk of progressing to a higher stage. Participants in stage 2 had a 54.5% (42 of 77) risk of progressing to a higher stage. Almost all participants (96.8%; 179 of 185) in stage 3 remained at that stage during follow-up (eTable 7 in the Supplement).

We also performed longitudinal analysis using follow-up data at 2 years, 4 years, and 6 years after baseline (Table 3). Transitions were more common at longer follow-up times. For example, participants in stage 2 at baseline had a 38% risk for progression to stage 3 at 2 years, a 59% risk for progression to stage 3 at 4 years, and a 90% risk for progression to stage 3 at 6 years.

Replication Cohort

In the 474 participants in the replication cohort, 267 (56.3%) were classified as stage 0, 14 (3.0%) as stage 1, 39 (8.2%) as stage 2, 146 (30.1%) as stage 3, and the classification algorithm failed in 8 participants (1.7%). The stage characteristics resembled the ADNI results, including distributions between diagnostic groups (CU: stage 0, 68.3%; stage 1, 3.3%; stage 2, 8.2%; stage

3, 19.0%; and unstageable, 1.3%; MCI: stage 0, 34.5%; stage 1, 2.4%; stage 2, 8.3%; stage 3, 52.4%; unstageable, 2.4%; eTable 8 in the Supplement), and association with MMSE score, which declined in stage 3 ($P < .001$ for baseline MMSE and rates of MMSE in stage 0 vs stage 3; eTable 9 in the Supplement). Slight increases in CSF tau markers were seen already at stage 1 (CSF T-tau: stage 0 vs stage 1, $P < .001$; CSF P-tau, stage 0 vs stage 1, $P = .001$).

Biological Pathways

A machine learning model classified tissue samples extracted from the brain as belonging to early, intermediate, or late composite regions with a cross-validation–balanced accuracy of 72% (precision, 78%; recall, 74%; Figure 2A, C), and performed similarly on left-out testing data (cross-validation–balanced accuracy, 67%; precision, 70%; recall, 70%; Figure 2B, C). This suggests the presence of a molecular signal that strongly overlaps with the regions identified from the previous analyses. eTable 10 in the Supplement lists significantly enriched biological pathways inversely associated with the regions (family-wise error rate $q < 0.1$). A central cluster of enriched pathways emerged associated with voltage-gated ion channel activity but also included subclusters of pathways associated with neuropeptide signaling, glutamate signaling, vasodilation, and lipid transportation, among other pathways (Figure 2D).

Discussion

We present a longitudinally valid staging system for ^{18}F-florbetapir PET, which may be used to monitor patients throughout a spatiotemporal Aβ pattern during the course of AD. A key aspect was the integration of CSF Aβ42 and ^{18}F-florbetapir PET data to construct (but not apply) the system. This integration built on previous observations that some participants have pathologic CSF Aβ42 concentrations without pathologic Aβ PET uptake,[7,27] which is associated with a greater risk for future Aβ,[8,9] and which may be used to identify Aβ starting regions.[10] The 4 stages had different characteristics, and were associated with clinical progression, in which symptoms often appeared in stages 2 and 3, but some people remain cognitively unimpaired even in stage 3. Cerebrospinal fluid concentrations of Aβ42 dropped in stage 1, P-tau levels increased in stage 1 and CSF T-tau levels increased in stage 2, cognitive decline accelerated in stage 2, and atrophy accelerated in stage 3, findings that are congruent with a proposed temporal evolution of biomarker changes in AD.[28]

The system had longitudinal validity, because each consecutive stage was associated with a risk of progression to a higher stage. Reversal to a lower stage, indicating system instability, was rare (0.9%). The risks differed from the 2-year follow-up to the 6-year follow-up, especially for stage 1, which was particularly dynamic, and quickly transitioned into higher stages. These findings may partly explain why few participants were classified as stage 1. After approximately 6 years, almost all participants in stages 1 and 2 at baseline had progressed to stage 3.

The regions in stage 1 and stage 3 are in agreement with the previously identified early and late Aβ-accumulating regions using a smaller data set.[10] Our system is also in agreement with the regional temporal Aβ pattern found in autosomal dominant AD using another amyloid PET tracer (^{11}C-Pittsburgh compound B) and a completely different methodology.[29] In that study, the earliest changes were seen in the precuneus, posterior cingulate, medial orbitofrontal cortices and the last regions to start accumulating Aβ were the sensorimotor, lingual, pericalcarine, and cuneus cortices. There are also similarities between our system and the neuropathologic findings by Braak and Braak,[3] in which the last cortical areas affected by Aβ were the sensorimotor area and parts of the occipital lobe, similar to our stage 3. The first regions affected according to Braak and Braak[3] included the medial orbitofrontal cortex, which appear in our stage 1. However, we also found that the precuneus, posterior cingulate, and isthmus cingulate cortices are among the first regions affected by Aβ fibrils, which is different from what is presented in both the Braak and Braak[3] (based on 83 patients) and the Thal (based on 51 patients) staging systems,[4] but, as presented above, is in agreement with Aβ PET findings from autosomal dominant AD.[29] One reason for differences with neuropathology may be that our model is based on ^{18}F-florbetapir PET, which mainly detects core and neuritic plaques, and to a lesser degree diffuse plaques.[5] Further, neuropathology-based studies are cross-sectional, assess a limited number of preselected brain regions (often not including posterior and isthmus cingulate), and seldom include many hundreds of patients spanning from CU to AD dementia.

Several key findings were validated in BioFINDER, using another PET tracer (^{18}F-flutemetamol) and CSF assay (Elecsys Aβ42). In the ADNI, 98.4% of participants could be unambiguously staged and in BioFINDER, 98.3% could be unambiguously staged. The distributions of stages were also similar, with stage 0 dominating among CU control participants, and stage 3 being much more common among MCI. Stage 1 was rare (CU: ADNI, 3.6%; BioFINDER, 3.3%; MCI: ADNI, 2.6%; BioFINDER, 2.4%), followed by stage 2 (CU: ADNI, 7.9%; BioFINDER, 8.2%; MCI: ADNI, 13.8%; BioFINDER, 8.3%). Changes in CSF P-tau were significant in stage 1 in both BioFINDER and in the ADNI. CSF T-tau changed in stage 1 in BioFINDER and in stage 2 in the ADNI. Temporal cortical thickness changed in stage 3 in the ADNI, with a similar trend in BioFINDER. In both cohorts, significant changes in MMSE score were seen at stage 3.

We also found strong differences in gene expression between the different stage composites, in particular for genes related to voltage-gated ion channel activity. Ion channel regulation has been linked to amyloid precursor protein,[30] β-site APP cleaving enzyme 1 (BACE1) function,[31] and Aβ accumulation.[32] These findings provide biological validation of the staging system and also hint at mechanisms that may underlie the regional selective vulnerability to Aβ pathology.

This study differs from another recently suggested Aβ PET staging model by Grothe et al.[33] Differences include that we

leveraged both PET and CSF Aβ biomarkers to highlight regions that are involved early; brain atlases (Grothe et al used the Harvard-Oxford atlas whereas we used the Desikan-Killany atlas); grouping of regions (Grothe et al grouped regions into quartiles, based on the ranks for how often the regions were abnormal in a cross-sectional setting, whereas our composites were identified by comparing rates of ^{18}F-florbetapir); cutoffs (Grothe et al used the same cutoff for Aβ positivity in all regions, whereas we used different cutoffs for different regions); counts for positivity (Grothe et al required more than 50% of the included number of regions in a stage to be positive for that stage to be counted as positive, whereas we used composites adjusted for the voxel counts); and validation (we validated the results longitudinally and in an independent cohort using another amyloid PET tracer). Despite these differences, there are also similarities between the results, emphasizing that different approaches may give partly converging results.

Limitations

Our study has limitations. The replication cohort had only cross-sectional PET data, so longitudinal transitions must be validated further. It is also possible that there is variability within some of the stages that could not be detected by our approach of contrasting CSF/PET groups. We used CSF Aβ42 alone, rather than adjusting for CSF Aβ40, which may give closer associations with amyloid PET.[34] This was because the staging system was based on a likely informative discordance between CSF Aβ42 and amyloid PET.[7,8,10]

Conclusions

We describe an Aβ PET staging system that may be useful for early diagnosis, drug development, and to study disease mechanisms. Future studies can further investigate the regional vulnerability that underlies the stages.

ARTICLE INFORMATION

Accepted for Publication: May 30, 2019.

Published Online: July 17, 2019. doi:10.1001/jamaneurol.2019.2214

Author Contributions: Dr Mattson had full access to all of the data in the study and takes responsibility for the integrity of the data and the accuracy of the data analysis. Drs Mattsson and Palmqvist contributed equally to the study.
Concept and design: Mattsson, Palmqvist, Hansson.
Acquisition, analysis, or interpretation of data: All authors.
Drafting of the manuscript: Mattsson, Palmqvist, Vogel.
Critical revision of the manuscript for important intellectual content: Palmqvist, Stomrud, Vogel, Hansson.
Statistical analysis: Mattsson, Palmqvist, Vogel.
Obtained funding: Mattsson, Palmqvist, Hansson.
Administrative, technical, or material support: Vogel, Hansson.
Supervision: Hansson.

Conflict of Interest Disclosures: Dr Mattsson reported being a consultant for the Alzheimer's Disease Neuroimaging Initiative (ADNI). Dr Hansson reported nonfinancial support from GE Healthcare, grants from Roche, and nonfinancial support from AVID Radiopharmaceuticals outside the submitted work and research support (for his institution) from Roche, GE Healthcare, Biogen, AVID Radiopharmaceuticals, Fujirebio, and Euroimmun; in the past 2 years, he has received consultancy/speaker fees paid to his institution from Biogen, Roche, and Fujirebio. No other disclosures were reported.

Funding/Support: Data collection and sharing for this project was were funded by the ADNI (National) Institutes of Health (grant U01 AG024904) and DOD ADNI (Department of Defense award W81XWH-12-2-0012). The Alzheimer's Disease Neuroimaging Initiative is funded by the National Institute on Aging, the National Institute of Biomedical Imaging and Bioengineering, and generous contributions from AbbVie, Alzheimer's Association; Alzheimer's Drug Discovery Foundation; Araclon Biotech; BioClinica, Inc; Biogen; Bristol-Myers Squibb Company; CereSpir, Inc; Cogstate; Eisai, Inc; Elan Pharmaceuticals, Inc; Eli Lilly and Company; EuroImmun; F. Hoffmann-La Roche, Ltd and its affiliated company Genentech, Inc; Fujirebio; GE Healthcare; IXICO, Ltd; Janssen Alzheimer Immunotherapy Research & Development, LLC; Johnson & Johnson Pharmaceutical Research & Development, LLC; Lumosity; Lundbeck; Merck & Co, Inc; Meso Scale Diagnostics, LLC; NeuroRx Research; Neurotrack Technologies; Novartis Pharmaceuticals Corporation; Pfizer, Inc; Piramal Imaging; Servier; Takeda Pharmaceutical Company; and Transition Therapeutics. The Canadian Institutes of Health Research is providing funds to support ADNI clinical sites in Canada. Private sector contributions are facilitated by the Foundation for the National Institutes of Health (http://www.fnih.org). The grantee organization is the Northern California Institute for Research and Education, and the study is coordinated by the Alzheimer's Therapeutic Research Institute at the University of Southern California. ADNI data are disseminated by the Laboratory for Neuroimaging at the University of Southern California. Work at the authors' research center was promoted by generous support from the Wallenberg Center for Molecular Medicine, Lund University, Lund, Sweden, European Research Council, the Swedish Research Council, the Knut and Alice Wallenberg foundation, the Marianne and Marcus Wallenberg foundation, the Strategic Research Area MultiPark (Multidisciplinary Research in Parkinson's disease) at Lund University, the Swedish Alzheimer Foundation, the Swedish Brain Foundation, The Parkinson foundation of Sweden, The Parkinson Research Foundation, the Skåne University Hospital Foundation, and the Swedish federal government under the ALF agreement.

Role of the Funder/Sponsor: The funders had no role in the design and conduct of the study; collection, management, analysis, and interpretation of the data; preparation, review, or approval of the manuscript; and decision to submit the manuscript for publication.

Meeting Presentation: This paper was presented at the Alzheimer's Association International Conference; July 17, 2019; Los Angeles, California.

Data Sharing Statement: Data used in preparation of this article were obtained from the ADNI database (http://adni.loni.usc.edu). As such, the investigators within the ADNI contributed to the design and implementation of ADNI and provided data but did not participate in analysis or writing of this report. A complete listing of the ADNI investigators can be found at: http://adni.loni.usc.edu/wp-content/uploads/how_to_apply/ADNI_Acknowledgement_List.pdf.

REFERENCES

1. Jack CR Jr, Wiste HJ, Weigand SD, et al. Amyloid-first and neurodegeneration-first profiles characterize incident amyloid PET positivity. *Neurology*. 2013;81(20):1732-1740. doi:10.1212/01.wnl.0000435556.21319.e4

2. Villemagne VL, Burnham S, Bourgeat P, et al; Australian Imaging Biomarkers and Lifestyle (AIBL) Research Group. Amyloid β deposition, neurodegeneration, and cognitive decline in sporadic Alzheimer's disease: a prospective cohort study. *Lancet Neurol*. 2013;12(4):357-367. doi:10.1016/S1474-4422(13)70044-9

3. Braak H, Braak E. Neuropathological stageing of Alzheimer-related changes. *Acta Neuropathol*. 1991;82(4):239-259. doi:10.1007/BF00308809

4. Thal DR, Rüb U, Orantes M, Braak H. Phases of A beta-deposition in the human brain and its relevance for the development of AD. *Neurology*. 2002;58(12):1791-1800. doi:10.1212/WNL.58.12.1791

5. Clark CM, Pontecorvo MJ, Beach TG, et al; AV-45-A16 Study Group. Cerebral PET with florbetapir compared with neuropathology at autopsy for detection of neuritic amyloid-β plaques: a prospective cohort study. *Lancet Neurol*. 2012;11(8):669-678. doi:10.1016/S1474-4422(12)70142-4

6. Ikonomovic MD, Buckley CJ, Heurling K, et al. Post-mortem histopathology underlying β-amyloid PET imaging following flutemetamol F 18 injection. *Acta Neuropathol Commun*. 2016;4(1):130. doi:10.1186/s40478-016-0399-z

7. Mattsson N, Insel PS, Donohue M, et al; Alzheimer's Disease Neuroimaging Initiative. Independent information from cerebrospinal fluid amyloid-β and florbetapir imaging in Alzheimer's

disease. *Brain*. 2015;138(pt 3):772-783. doi:10.1093/brain/awu367

8. Palmqvist S, Mattsson N, Hansson O; Alzheimer's Disease Neuroimaging Initiative. Cerebrospinal fluid analysis detects cerebral amyloid-β accumulation earlier than positron emission tomography. *Brain*. 2016;139(pt 4):1226-1236. doi:10.1093/brain/aww015

9. Vlassenko AG, McCue L, Jasielec MS, et al. Imaging and cerebrospinal fluid biomarkers in early preclinical Alzheimer disease. *Ann Neurol*. 2016;80(3):379-387. doi:10.1002/ana.24719

10. Palmqvist S, Schöll M, Strandberg O, et al. Earliest accumulation of β-amyloid occurs within the default-mode network and concurrently affects brain connectivity. *Nat Commun*. 2017;8(1):1214. doi:10.1038/s41467-017-01150-x

11. Petersen RC, Aisen PS, Beckett LA, et al. Alzheimer's Disease Neuroimaging Initiative (ADNI): clinical characterization. *Neurology*. 2010;74(3):201-209. doi:10.1212/WNL.0b013e3181cb3e25

12. Folstein MF, Folstein SE, McHugh PR. "Mini-mental state": a practical method for grading the cognitive state of patients for the clinician. *J Psychiatr Res*. 1975;12(3):189-198. doi:10.1016/0022-3956(75)90026-6

13. Morris JC. The Clinical Dementia Rating (CDR): current version and scoring rules. *Neurology*. 1993;43(11):2412-2414. doi:10.1212/WNL.43.11.2412-a

14. McKhann G, Drachman D, Folstein M, Katzman R, Price D, Stadlan EM. Clinical diagnosis of Alzheimer's disease: report of the NINCDS-ADRDA Work Group under the auspices of Department of Health and Human Services Task Force on Alzheimer's Disease. *Neurology*. 1984;34(7):939-944. doi:10.1212/WNL.34.7.939

15. Crane PK, Carle A, Gibbons LE, et al; Alzheimer's Disease Neuroimaging Initiative. Development and assessment of a composite score for memory in the Alzheimer's Disease Neuroimaging Initiative (ADNI). *Brain Imaging Behav*. 2012;6(4):502-516. doi:10.1007/s11682-012-9186-z

16. Gibbons LE, Carle AC, Mackin RS, et al; Alzheimer's Disease Neuroimaging Initiative. A composite score for executive functioning, validated in Alzheimer's Disease Neuroimaging Initiative (ADNI) participants with baseline mild cognitive impairment. *Brain Imaging Behav*. 2012;6(4):517-527. doi:10.1007/s11682-012-9176-1

17. Shaw LM, Vanderstichele H, Knapik-Czajka M, et al; Alzheimer's Disease Neuroimaging Initiative. Cerebrospinal fluid biomarker signature in Alzheimer's Disease Neuroimaging Initiative subjects. *Ann Neurol*. 2009;65(4):403-413. doi:10.1002/ana.21610

18. Desikan RS, Ségonne F, Fischl B, et al. An automated labeling system for subdividing the human cerebral cortex on MRI scans into gyral based regions of interest. *Neuroimage*. 2006;31(3):968-980. doi:10.1016/j.neuroimage.2006.01.021

19. Jack CR Jr, Wiste HJ, Weigand SD, et al. Different definitions of neurodegeneration produce similar amyloid/neurodegeneration biomarker group findings. *Brain*. 2015;138(Pt 12):3747-3759. doi:10.1093/brain/awv283

20. Landau SM, Mintun MA, Joshi AD, et al; Alzheimer's Disease Neuroimaging Initiative. Amyloid deposition, hypometabolism, and longitudinal cognitive decline. *Ann Neurol*. 2012;72(4):578-586. doi:10.1002/ana.23650

21. Landau SM, Fero A, Baker SL, et al. Measurement of longitudinal β-amyloid change with ^{18}F-florbetapir PET and standardized uptake value ratios. *J Nucl Med*. 2015;56(4):567-574. doi:10.2967/jnumed.114.148981

22. Landau S. Jagust W Florbetapir processing methods. Alzheimer's Disease Neuroimaging Initiative. https://adni.bitbucket.io/reference/docs/UCBERKELEYAV45/ADNI_AV45_Methods_JagustLab_06.25.15.pdfhttps://adni.bitbucket.io/reference/docs/UCBERKELEYAV45/ADNI_AV45_Methods_JagustLab_06.25.15.pdf. Revised June 25, 2015. Accessed June 28, 2019.

23. Palmqvist S, Zetterberg H, Blennow K, et al. Accuracy of brain amyloid detection in clinical practice using cerebrospinal fluid β-amyloid 42: a cross-validation study against amyloid positron emission tomography. *JAMA Neurol*. 2014;71(10):1282-1289. doi:10.1001/jamaneurol.2014.1358

24. Mattsson N, Insel PS, Palmqvist S, et al. Increased amyloidogenic APP processing in APOE ε4-negative individuals with cerebral β-amyloidosis. *Nat Commun*. 2016;7:10918. doi:10.1038/ncomms10918

25. Hansson O, Seibyl J, Stomrud E, et al; Swedish BioFINDER Study Group; Alzheimer's Disease Neuroimaging Initiative. CSF biomarkers of Alzheimer's disease concord with amyloid-β PET and predict clinical progression: a study of fully automated immunoassays in BioFINDER and ADNI cohorts. *Alzheimers Dement*. 2018;14(11):1470-1481. doi:10.1016/j.jalz.2018.01.010

26. Subramanian A, Tamayo P, Mootha VK, et al. Gene set enrichment analysis: a knowledge-based approach for interpreting genome-wide expression profiles. *Proc Natl Acad Sci U S A*. 2005;102(43):15545-15550. doi:10.1073/pnas.0506580102

27. Fagan AM, Mintun MA, Shah AR, et al. Cerebrospinal fluid tau and ptau(181) increase with cortical amyloid deposition in cognitively normal individuals: implications for future clinical trials of Alzheimer's disease. *EMBO Mol Med*. 2009;1(8-9):371-380. doi:10.1002/emmm.200900048

28. Jack CR Jr, Knopman DS, Jagust WJ, et al. Hypothetical model of dynamic biomarkers of the Alzheimer's pathological cascade. *Lancet Neurol*. 2010;9(1):119-128. doi:10.1016/S1474-4422(09)70299-6

29. Gordon BA, Blazey TM, Su Y, et al. Spatial patterns of neuroimaging biomarker change in individuals from families with autosomal dominant Alzheimer's disease: a longitudinal study. *Lancet Neurol*. 2018;17(3):241-250. doi:10.1016/S1474-4422(18)30028-0

30. Liu C, Tan FCK, Xiao Z-C, Dawe GS. Amyloid precursor protein enhances Nav1.6 sodium channel cell surface expression. *J Biol Chem*. 2015;290(19):12048-12057. doi:10.1074/jbc.M114.617092

31. Lehnert S, Hartmann S, Hessler S, Adelsberger H, Huth T, Alzheimer C. Ion channel regulation by β-secretase BACE1 - enzymatic and non-enzymatic effects beyond Alzheimer's disease. *Channels (Austin)*. 2016;10(5):365-378. doi:10.1080/19336950.2016.1196307

32. Daschil N, Obermair GJ, Flucher BE, et al. CaV1.2 calcium channel expression in reactive astrocytes is associated with the formation of amyloid-β plaques in an Alzheimer's disease mouse model. *J Alzheimers Dis*. 2013;37(2):439-451. doi:10.3233/JAD-130560

33. Grothe MJ, Barthel H, Sepulcre J, Dyrba M, Sabri O, Teipel SJ; Alzheimer's Disease Neuroimaging Initiative. In vivo staging of regional amyloid deposition. *Neurology*. 2017;89(20):2031-2038. doi:10.1212/WNL.0000000000004643

34. Janelidze S, Zetterberg H, Mattsson N, et al; Swedish BioFINDER Study Group. CSF Aβ42/Aβ40 and Aβ42/Aβ38 ratios: better diagnostic markers of Alzheimer disease. *Ann Clin Transl Neurol*. 2016;3(3):154-165. doi:10.1002/acn3.274